Published in final edited form as:
J Neurosci Methods. 2008 August 15; 173(1): 20–26. doi:10.1016/j.jneumeth.2008.05.007.

Single-synapse ablation and long-term imaging in live *C. elegans*

Peter B. Allen†, **Allyson E. Sgro**†, **Daniel L. Chao**‡, **Byron E. Doepker**†, **J. Scott Edgar**†, **Kang Shen**‡, and **Daniel T. Chiu**†

† *Department of Chemistry, University of Washington, Box 351700, Seattle, WA 98195-1700, Tel: (206) 543-1655, E-mail: chiu@chem.washington.edu*

‡ *Department of Biological Sciences, Stanford University, 371 Serra Mall, Herrin Labs Room 144, Stanford, CA 94305-5020, Tel: 650-724-7975, Email: kangshen@stanford.edu*

Abstract

Synapses are individually operated, computational units for neural communication. To manipulate physically individual synapses in a living organism, we have developed a laser ablation technique for removing single synapses in live neurons in *C. elegans* that operates without apparent damage to the axon. As a complementary technique, we applied microfluidic immobilization of *C. elegans* to facilitate long-term fluorescence imaging and observation of neuronal development. With this technique, we directly demonstrated the existence of competition between developing synapses in the HSNL motor neuron.

Keywords

synapse; *C. elegans*; development; synaptogenesis; microfluidics; ablation; laser; LIF; imaging

Introduction

Synaptic changes are thought to be important to learning and memory. These changes can take the form of modulations of synaptic strength such as long-term potentiation (LTP) or depression (LTD), or the formation of new synapses and elimination of existing synapses (Geinisman et al., 1996; Toni et al., 1999) and the restructuring of the network topology (Maletic-Savatic et al., 1999), among other potential mechanisms. Behavorial studies show that nematode *C. elegans* exhibits multiple forms of learning (Hedgecock and Russell, 1975; Zhang et al., 2005). Cell biological studies suggest that synaptic structures change dynamically in response to environmental stimuli (Zhao and Nonet, 2000). Perturbations of sensory activity in *C. elegans*, for example, affect the maintenance of sensory axon morphology (well after initial development) that results in alterations of synapse morphology (Peckol et al., 1999). Furthermore, structural and functional parameters of synapses can be modified by adjacent synapses suggesting that interactions between synapses exist (Engert and Bonhoeffer, 1997; Harvey and Svoboda, 2007).

To study such remodeling of the topology and connectivity of the neuronal network, it would be useful to have a technique with which one can perturb the network with high spatiotemporal

Correspondence to: Daniel T. Chiu.

precision, then make a detailed recording of the remodeling and adaptation that the network subsequently undergoes. Here, we describe one such tool, where a tightly focused nanosecond laser pulse in the UV wavelength region is used to ablate a single synapse in live *C. elegans* with high spatiotemporal precision and without apparent damage to the axon; the axon is dimly but visibly fluorescent in many of the animals studied, and persists after ablation in the animals where we could see it initially. We also observe re-formation of synapses after synapse ablation, which again points to the integrity of the axon. Changes in network connectivity are monitored over long periods of time (hours) using fluorescence imaging. This technique combines recent advances in microscopy to achieve single-synapse ablation and in microfluidics for immobilizing *C. elegans* for long-term imaging.

The use of laser microsurgery to study cell lineage and neural development has a long history in the study of *C. elegans* and other organisms including *Drosophila* (Chang and Keshishian, 1996). In classic experiments, (Sulston and White, 1980) progenitor cells or neurons of interest (typically a few to tens of micrometers in size) were ablated and the effects on the development or behavior of the final organism were observed (Bargmann and Avery, 1995; Gray et al., 2005). With recent advances in microscopy –both in laser ablation and single-cell nanosurgery (Jeffries et al., 2007; Shelby et al., 2005; Sun and Chiu, 2004; Sun et al., 2004; Yanik et al., 2004) and in sensitive single-molecule imaging – it is now possible to improve the precision of single-pulse laser ablation from single cells to single synapses.

Once a desired perturbation has been made to the neuronal network, it is often desirable to image the long-term remodeling of the network. For example, time-lapse imaging of single mouse neurons in hippocampal slices shows directly that dendiritc spines generated after LTP can form new synapses (Nagerl et al., 2007), a finding that had been suggested by the increases in synaptic contacts observed in static electron microscopy studies (Knott et al., 2006). With the time-lapse experiment, however, it was possible to see directly the temporal stages of the synaptogenesis process and thus definitively show that new connections are formed between previously unconnected neurons. It has been difficult, however, to perform such long-term imaging experiments in live *C. elegans*, because worms cannot be immobilized for much longer than ½ hours with traditional techniques (e.g. with anesthetics or glue) without greatly affecting the health and viability of the worm.

To address this issue, we turn to several very recent developments in microfluidics where tailored microchannels were used to provide more control over the physical state of the worm during growth (Kim et al., 2007), and for short-term (Rohde et al., 2007) and long-term (Hulme et al., 2007) observation. In particular, we take advantage of the microfluidic clamp recently described by Whitesides and co-workers for the immobilization of *C. elegans* over long periods of time (days) (Hulme et al., 2007). In combination with sensitive fluorescence imaging, we were able to follow the growth and remodeling of single axons and synapses over hours.

We applied our technique to study the development of the HSNL motor neuron in *C. elegans*, which has been used as a model to understand synaptogenesis (Shen and Bargmann, 2003). It is known that HSNL elaborates a group of en passant synapses within a short segment of its axon near the vulval organ. This restricted subcellular distribution pattern of HSNL synapses results from initial synaptogenesis in a broader area followed by elimination of certain synapses (Ding et al., 2007). Molecular genetic studies suggest that two immunoglobulin superfamily proteins, SYG-1 and SYG-2, are essential for the appropriate subcellular localization and synaptic target selection of HSNL. SYG-2, which is expressed by the vulval epithelial cells, binds to SYG-1 on the HSNL neuron and localizes SYG-1 to the normal synaptic region where synapses sustain and grow. The synapses which do not co-localize with SYG-1 are eventually eliminated by ubiquitin-proteasome system. In *syg-1* or *syg-2* mutants, ectopic synapses failed to be eliminated; synapse formation at the normal location is drastically

reduced (Shen et al., 2004). These results hint that there are potential competitions between synapses during development and the growth of certain synapses might occur at the expense of other synapses. Direct evidence of such dynamic, competitive developmental processes requires time-lapse imaging experiments during the period of synapse competition and experimental approaches that would allow direct perturbation of synapses *in vivo*.

Prior to the development of this technique, we had to rescue animals from the slides to culture plates between imaging acquisitions. This greatly reduces the viability of the animals and limits the number of pictures taken to less than 3–4 in most cases (Ding et al., 2007). Here, we visualized directly the development of this neuron during synapse competition, and showed that HSNL forms numerous pre-synapses at early developmental stages and that continuous mobility and competition occurs at later stages as well, leading to the mature synaptic pattern. In addition, we used a tightly focused laser to artificially ablate specific synapses without severing the axon. We show that ablation of synapses in the normal (SYG-1 co-localized) region leads to ectopic synapses, a phenotype similar to that observed in *syg-1* and *syg-2* mutants. These results further prove that competition exists between developing synapses.

Materials and methods

Fabrication of PDMS microfluidic chips

Silicon masters that had features composed of SU-8 negative photoresist were fabricated using standard photolithography techniques (Duffy et al., 1998). Specifically, 40μm layer of photoresist was spin coated onto a silicon wafer and developed via UV exposure. Following photolithography, the master was exposed to tridecafluoro-1,1,2,2-tetrahydrooctyl-1-trichlorosilane vapour overnight to silanize the features, which facilitated mold release during replication of the polymer chips.

The microchannels were formed out of poly(dimethylsiloxane) (PDMS) via replica molding, where a 10:1 ratio of prepolymer to catalyst was poured on top of the silicon master, baked for 1 hour at 60 °C, and then cut out and removed from the master. Access holes were punched in the resulting PDMS slabs using a 16-gauge needle. The slabs were then permanently sealed to glass coverslips with oxygen plasma treatment.

C. elegans immobilization

To generate continuous fluid flow, lengths of polyethylene tubing (PE100, BD, Franklin Lakes, NJ) were inserted into the access holes, then attached to 30 ml syringes (BD, Franklin Lakes, NJ) so fluid could be introduced into the channels at a constant rate. Fluid flow was driven and controlled by a syringe pump (KD Scientific, Holliston, MA). *C. elegans* (strain *wyIs22* [*Punc-86::GFP::rab-3*]) were selected from growth plates and suspended in 0.1 M phosphate buffered saline (PBS). Initially the microfluidic channels were wetted with the same PBS and then the inlet tubing was removed from the chip and placed in the Eppendorf tube containing the worms. The *C. elegans*-containing PBS was withdrawn from the Eppendorf tube into the tubing using the withdraw mode of the syringe pump and then the tubing was re-inserted into the chip. *C. elegans* were introduced into the chip using the fast-forward feature of the syringe pump until multiple *C. elegans* were observed to be pinned in the tapered channels of the chip. In the vast majority of cases, the first worm to enter a channel blocked the buffer flow through that channel. As a result, subsequent worms flowed into other channels. This was sufficient to limit the channels to one worm unless two worms entered a channel virtually simultaneously. By keeping the number density of worms injected into the chip to a reasonable level, this possibility was mostly eliminated. After the introduction of multiple *C. elegans* into the tapered channels, the PBS flow rate was set to between 20 and 40 μl/min for the duration of the experiment.

Images were captured at 60-second intervals using a cooled CCD camera (Cascade 512b or Cascade 650 from Princeton Instruments, Trenton, NJ). The camera triggered the opening of a shutter, which resulted in illumination of the sample with 488 nm light in epifluorescence mode for 50–100 ms per image; this procedure minimizes photobleaching of the sample. The magnification was either 30× or 100×. Captured images were assembled into a time-lapse video using Mathematica (Wolfram Research, Champaign, IL) and Labview software (National Instruments, Austin, TX).

Synapse ablation

A 355 nm pulsed UV laser (Minilite from Continuum, Santa Clara, CA) was focused at the object plane of a 100× UV transmitting objective (Superfluor, Nikon, Tokyo, Japan). Under epi-illumination with a 488 nm blue laser (Sapphire, Coherent, Santa Clara, CA), we visualized the punctuate synapses at the target region of the HSNL motor neuron, which was genetically modified to express GFP at its synapses. To ablate the synapses, we typically used 10–20 single laser pulses (~ 3ns pulse and 1–10 μJ per pulse), because the laser focus is smaller than the synapses. For these single-synapse ablation experiments, the worms were either held in place and clamped down by the microchannels followed by long-term imaging, or anaesthetized with levamisole then returned to the individual growth plates.

For studying the morphology of HSNL motor synapse, we used an integrated *wyIs22* strain [*Punc-86::GFP::rab-3*], where after ablation, we returned the worms to the growth plates and let the worm/synapse develop for 2–3 hours. Approximately 80% of the worms were viable after 2–3 hours of development. The same worms were imaged again under excitation with the 488 nm laser. The location and morphology of the HSNL motor synapses and in particular the presence or absence of ectopic synapses were noted. We included a total of 31 L4 animals and 22 YA animals for analysis.

Results and discussion

Single-synapse ablation and long-term imaging

Figure 1A schematically illustrates our experimental setup and approach, in which worms immobilized in the microchannels were placed onto an inverted microscope for ablation and imaging. Because the height of the microchannels is greater than their widths, the confined worms orient themselves such that they are rotated onto their sides (Figure 1B top panel); the middle panel in Figure 1B shows a bright-field image of an immobilized worm. In addition to long-term immobilization and fluorescence imaging of live worms, we were also able to achieve single-pulse laser ablation with high spatial precision. The bottom panel of Figure 1B shows the selective ablation of a single 500 nm-diameter bead in close proximity (~ 300nm) to other beads with a single ~3ns laser pulse at 355nm.

Figure 2A shows in more detail the microfluidic channel design (worm corral) that we used, which contained a tapered region in which worms at the desired developmental stage were trapped because they were unable to pass the tapered and constricted channel except at extreme pressures. In more detail, this worm-corral design has a two-stage taper. In the first stage, the corral has a wide opening to encourage the flow of worm-bearing buffer into the inlets. In the second stage, the channels have a shallow taper that linearly decreases from a width of 100 μm to a narrow passage of 8μm over a distance of 0.5 mm. The shallow taper helped prevent the worm from moving against the flow.

Figure 2B shows a representative series of images of the early development of the HSNL motor neuron in a L4 stage specimen over ~1.5 hours. Here, the punctuate spots representing the trafficking of synaptic proteins are visualized with the GFP::RAB-3 fusion protein. In this time

sequence, the neuron can be seen to extend several pre-assembled punctuate spots containing GFP::RAB-3. After traveling out toward the region of interest, several of the spots fade in a manner consistent with early organizing events of the wild type (WT) synapses.

One possible concern in such long-term immobilization and imaging experiments is the effects spatial confinement has on the worms. Previous studies using a similar microfluidic trapping system showed that *C. elegans* tolerates these conditions well, where survival of worms was reported to be 100 % for up to 9 days (Hulme et al., 2007). We found that after being confined to the trapped region for a time (minutes) then being pushed through the narrow orifice (which is elastomeric, and stretched to allow the worm to pass), the worms appeared stiff and maintained a straight posture for a few minutes after being freed (data not shown). It seems possible that the normal muscle actions of locomotion are inhibited during close confinement, which may contribute to the high survivability.

In our long-term fluorescence imaging experiments, we observed that in most cases, the worms responded dramatically to illumination with 488 nm (blue) light. Under strong illumination with white light, the worm would be stable for hours, but with intermittent sub-milliwatt blue illumination, the worm 'panicked' and struggled in the microfluidic channel. This makes time lapse imaging more challenging in this mode. Several small changes helped to offset this effect. First, by using a higher magnification objective and a smaller field of view, we were able to limit the area of illumination to a select region of the worm. Although the response was often still present, it seemed less prevalent. Additionally, the shallow taper of the corral limited the ability of the worm to move in its struggles. Finally, simultaneous illumination with 633 nm light seemed to reduce the response.

Normal development of the HSNL motor neuron

To follow the early stages of synaptogenesis that the HSNL neuron undergoes, we selected worms at the L4 development stage. Here, we take advantage of the ability to label a single neuron and its synapses by fusing GFP to the desired synapse-specific proteins (Schaefer et al., 2000). Figure 2B shows a representative series of time lapse images, which show some pre-synaptic dynamic localization of GFP::RAB-3 puncta. The series shows some of the dynamic trafficking events prior to the subtractive processes shown in previous studies (Ding et al., 2007).

Additionally, the specimen observed from the young adult (YA) stage into early maturity over the course of 4 hours (Figure 3) showed continuous dynamic changes even after the mature pattern of synaptic puncta were established. These results seem to indicate that even after the mature pattern is formed (the morphology is consistent with the adult pattern at 55 minutes) the synapses continue to rearrange in a dynamic manner within the region of the WT puncta. In particular, between 136 to 220 minutes a single punctum appears at the ventral side of the features and is arranged toward the anterior as is shown by arrows in Figure 3.

In previous static snapshots of the developing HSNL neuron taken at various discrete time points, ectopic HSNL synapses anterior of the vulva are frequently seen in L4 staged WT worms but rarely observed in WT, YA animals. In *syg-1* and *syg-2* mutant animals, anterior ectopic punta are observed in all stages (Ding et al., 2007). It is plausible that anterior ectopic puncta also exist in WT, YA animals, but are quickly eliminated. Our time lapse experiments suggest continual adjustment of the active synapses, but ectopic synapses do not appear even transiently in this YA animal.

Effects of synapse ablation on the development of the HSNL neuron

Next, we studied the effect of disrupting the synapse at the crucial point of its development where it becomes committed to its target. We tested the hypothesis that proper synaptic targeting occurred at the L4-YA transition and that it occurred between the presynapse and cells in its immediate vicinity. After ablating the HSNL synapses and allowing time for further development of the HSNL neuron, some 35 % of the worms at L4 stage of development subjected to ablation showed ectopic synapses compared to only 4 % of the control group (YA) subjected to the same procedure after complete development of the neuron.

Figure 4A shows a typical morphology of a YA prior to ablation (frames 1–3 are bright field, bright field with fluorescence, and fluorescence only images, respectively). Figure 4A shows the ablation process in frames 3–13. Frame 14 shows the cell body (which is at a different focal plane than the synapses) after ablation, and frame 15 is the bright-field image after ablation. Frame 16 shows the re-appearance of the synapses (small arrows) at the normal synaptic location 2–3 hours after ablation; here, we observed no ectopic synapses at the location indicated (big arrow). Figure 4B and 4C show the pre- and post-ablation of another, younger worm at the L4 development stage. Figure 4D shows the ectopic synapses that formed after ablation of the original synapses (indicated with an arrow), which contrasts with the result observed with YA worms.

Although the precise character of the damage caused by the UV laser pulse is not known, proteins present at the focal region are known to degrade and take on inactive forms upon intense laser irradiation (Kaehr et al., 2004). It is therefore reasonable to assume that the damage to the ablated region was severe and certainly was sufficient to disrupt the signaling molecules at the synapse.

In these experiments, we chose individuals without ectopic synapses for ablation, but after ablation ectopic synapses appeared over the ensuing hours. The high frequency of this outcome in L4 stage worms relative to the YA cases is evidently due to the timing of the event. At the YA stage, the deterministic interactions that commit the synapses to their proper targets have already occurred and the worm no longer seeks to form more synapses that could end up in aberrant locations. Those events occur near to the chosen time at which we ablated the synapses in the L4 animals. From this, we believe that ablation just before the events of interest produced the cases where ectopic synapses were observed. Consistent with this observation, SYG-2 expression peaks in the L4 stage and is down-regulated in adults (Shen et al., 2004). The observation of ectopic synapses in these circumstances (showing the evident lack of subtractive processes) supports the hypothesis that competition between developing synapses during a defined time window shapes the final synaptic pattern.

Conclusions

This paper demonstrates a new technique to probe the development and remodeling of synaptic connections in live *C. elegans*. The results with respect to the HSNL motor neuron support the view presented by recent findings (Ding et al., 2007) that the neuron develops synapses through a subtractive process wherein a set of potential synapses are generated, and the subset of proper synapses are carried into the mature individual while others are eliminated in a dynamic process. The synapse elimination process takes place when signaling events involving SYG-1 and SYG-2 occur between target and presynaptic cells (Ding et al., 2007). When the site of these events is disrupted before the event is complete, synapses are found later in ectopic areas. We made observations of events in this process over a period of several hours and confirmed observations of apparent dynamic processes in which multiple possible clusters of synaptic vesicle proteins are observed initially, but only appropriate synapses are retained into the later parts of the developmental cycle. Additionally, longer observations of the synapse in its final,

determined location showed continuing dynamic activity including the generation of new, properly located synapses. The synaptic ablation experiments directly showed that there was competition between the synapses formed at the normal location and the synapses formed at the ectopic locations. The difference in the plasticity (taken as the ability to recover proper or form new synapses) after laser ablation at L4 and YA stage suggest that the competition occurs during the L4-YA transition.

Synaptic ablation and long-term imaging yield direct information that is not accessible from composite analysis of the development of many individuals. This technique does not distinguish, for example, between the possibility of the HSNL motor neuron targeting apparatus being on the neuron or the muscle side of the synapse; it only localizes it to a region in space and time. Nonetheless, approach allows one to study directly the cause-and-effect relationship between the structure and function of the neuronal network, which we believe complements the inferences drawn from the powerful genetic and biochemical techniques currently in use for studying the neural network of *C. elegans*.

Acknowledgements

Peter Allen thanks the NSF for their support through the graduate research fellowship. Byron Doepker thanks the Mary Gates foundation for an undergraduate research grant. This research was supported by the NIH and Keck Foundation.

References

Bargmann CI, Avery L. Laser killing of cells in Caenorhabditis elegans. Meth Cell Biol 1995;48:225–50.

Chang TN, Keshishian H. Laser Ablation of Drosophila Embryonic Motoneurons Causes Ectopic Innervation of Target Muscle Fibers. J Neurosci 1996;16:5715–26. [PubMed: 8795627]

Ding M, Chao D, Wang G, Shen K. Spatial Regulation of an E3 Ubiquitin Ligase Directs Selective Synapse Elimination. Science 2007;317:947–51. [PubMed: 17626846]

Duffy DC, McDonald JC, Schueller OJA, Whitesides GM. Rapid Prototyping of Microfluidic Systems in Poly(dimethylsiloxane). Anal Chem 1998;70:4974–84.

Engert F, Bonhoeffer T. Synapse specificity of long-term potentiation breaks down at short distances. Nature 1997;388:279–84. [PubMed: 9230437]

Geinisman Y, Detoledo-Morrell L, Morrell F, Persina IS, Beatty MA. Synapse restructuring associated with the maintenance phase of hippocampal long-term potentiation. J Comp Neurol 1996;368:413–23. [PubMed: 8725348]

Gray JM, Hill JJ, Bargmann CI. Inaugural Article: A circuit for navigation in Caenorhabditis elegans. PNAS 2005;102:3184–91. [PubMed: 15689400]

Harvey CD, Svoboda K. Locally dynamic synaptic learning rules in pyramidal neuron dendrites. Nature 2007;450:1195–200. [PubMed: 18097401]

Hedgecock EM, Russell RL. Normal and mutant thermotaxis in the nematode Caenorhabditis elegans. PNAS 1975;72:4061–5. [PubMed: 1060088]

Hulme SE, Shevkoplyas SS, Apfeld J, Fontana W, Whitesides GM. A microfabricated array of clamps for immobilizing and imaging C. elegans. Lab Chip 2007;7:1515–23. [PubMed: 17960280]

Jeffries GD, Edgar JS, Zhao Y, Shelby JP, Fong C, Chiu DT. Using polarization-shaped optical vortex traps for single-cell nanosurgery. Nano letters 2007;7:415–20. [PubMed: 17298009]

Kaehr B, Allen R, Javier DJ, Currie J, Shear JB. Guiding neuronal development with in situ microfabrication. PNAS 2004;101:16104–8. [PubMed: 15534228]

Kim N, Dempsey CM, Zoval JV, Sze J-Y, Madou MJ. Automated microfluidic compact disc (CD) cultivation system of Caenorhabditis elegans. Sens Actuators, B 2007;122:511–8.

Knott GW, Holtmaat A, Wilbrecht L, Welker E, Svoboda K. Spine growth precedes synapse formation in the adult neocortex in vivo. Nat Neurosci 2006;9:1117–24. [PubMed: 16892056]

Maletic-Savatic M, Malinow R, Svoboda K. Rapid Dendritic Morphogenesis in CA1 Hippocampal Dendrites Induced by Synaptic Activity. Science 1999;283:1923–7. [PubMed: 10082466]

Nagerl UV, Kostinger G, Anderson JC, Martin KAC, Bonhoeffer T. Protracted synaptogenesis after activity-dependent spinogenesis in hippocampal neurons. J Neurosci 2007;27:8149–56. [PubMed: 17652605]

Peckol EL, Zallen JA, Yarrow JC, Bargmann CI. Sensory activity affects sensory axon development in C. elegans. Development 1999;126:1891–902. [PubMed: 10101123]

Rohde CB, Zeng F, Gonzalez-Rubio R, Angel M, Yanik MF. Microfluidic system for on-chip high-throughput whole-animal sorting and screening at subcellular resolution. PNAS 2007;104:13891–5. [PubMed: 17715055]

Schaefer AM, Hadwiger GD, Nonet ML. rpm-1, A Conserved Neuronal Gene that Regulates Targeting and Synaptogenesis in C.elegans. Neuron 2000;26:345–56. [PubMed: 10839354]

Shelby JP, Edgar JS, Chiu DT. Monitoring cell survival after extraction of a single subcellular organelle using optical trapping and pulsed-nitrogen laser ablation. Photochem Photobiol 2005;81:994–1001. [PubMed: 15850426]

Shen K, Bargmann CI. The Immunoglobulin Superfamily Protein SYG-1 Determines the Location of Specific Synapses in C. elegans. Cell 2003;112:619–30. [PubMed: 12628183]

Shen K, Fetter RD, Bargmann CI. Synaptic specificity is generated by the synaptic guidepost protein SYG-2 and its receptor, SYG-1. Cell 2004;116:869–81. [PubMed: 15035988]

Sulston JE, White JG. Regulation and cell autonomy during postembryonic development of Caenorhabditis elegans. Developmental Biology 1980;78:577–97. [PubMed: 7190941]

Sun B, Chiu DT. Synthesis, loading, and application of individual nanocapsules for probing single-cell signaling. Langmuir 2004;20:4614–20. [PubMed: 15969173]

Sun B, Lim DS, Kuo JS, Kuyper CL, Chiu DT. Fast initiation of chemical reactions with laser-induced breakdown of a nanoscale partition. Langmuir 2004;20:9437–40. [PubMed: 15491172]

Toni N, Buchs PA, Nikonenko I, Bron CR, Muller D. LTP promotes formation of multiple spine synapses between a single axon terminal and a dendrite. Nature 1999;402:421–5. [PubMed: 10586883]

Yanik MF, Cinar HN, Chisholm AD, Jin Y, Ben-Yakar A. Neurosurgery: Functional regeneration after laser axotomy. Nature 2004;432:822. [PubMed: 15602545]

Zhang Y, Lu H, Bargmann CI. Pathogenic bacteria induce aversive olfactory learning in Caenorhabditis elegans. Nature 2005;438:179–84. [PubMed: 16281027]

Zhao H, Nonet ML. A retrograde signal is involved in activity-dependent remodeling at a C. elegans neuromuscular junction. Development 2000;127:1253–66. [PubMed: 10683178]

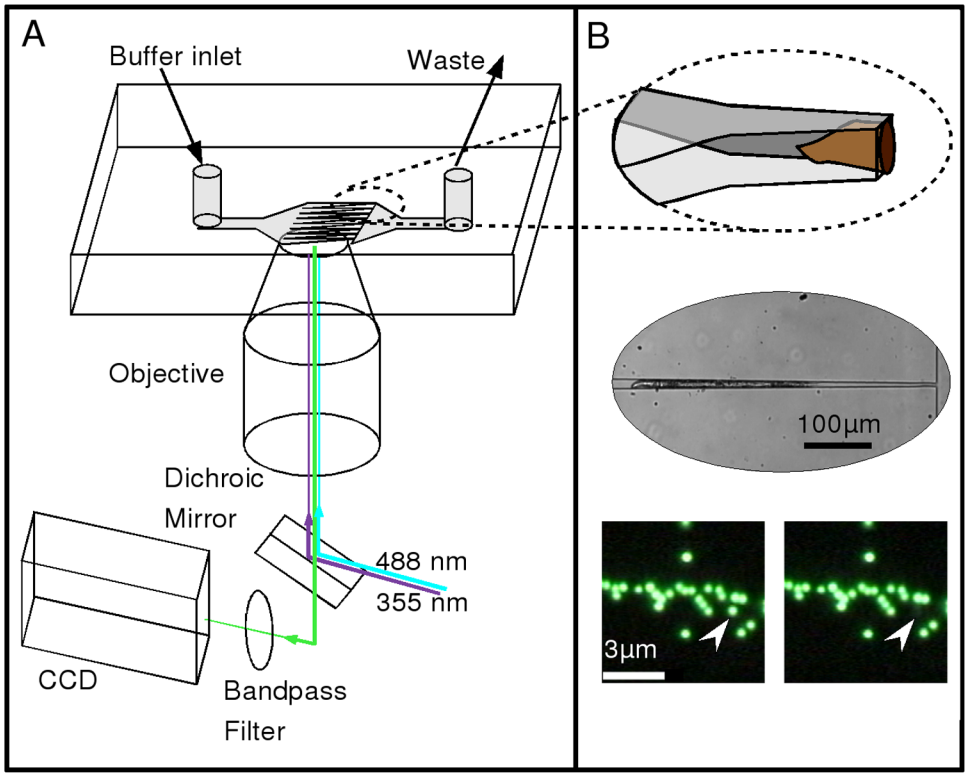

Figure 1.

Overview of the experimental design. (A) Schematic illustrating the arrangement of the optical setup and microfluidic chip. Buffer flow is from left to right in the direction of the taper, such that worms are push towards the channel constrictions. Two laser sources, a blue (488 nm, CW) and an ultraviolet (355 nm, ~ 3ns pulse), are reflected from a dichroic mirror into the back aperture of a microscope objective lens and directed into the sample for fluorescence excitation and ablation, respectively. Fluorescence is collected and imaged with a CCD camera. (B) Top image: an illustration showing the details of the microfluidic system and the captured worm. The channels narrow to a final width of 8µm while maintaining a constant height of ~ 30µm. As a result, the worms tend to be rotated onto their side, as shown. Middle image: A bright-field image showing a worm trapped in the narrow region of the tapered channel. Bottom images: A before and after picture showing the selective ablation of a single 500 nm bead (indicated by arrow) in close proximity to other beads. The scale bar in the left image represents 3 µm.

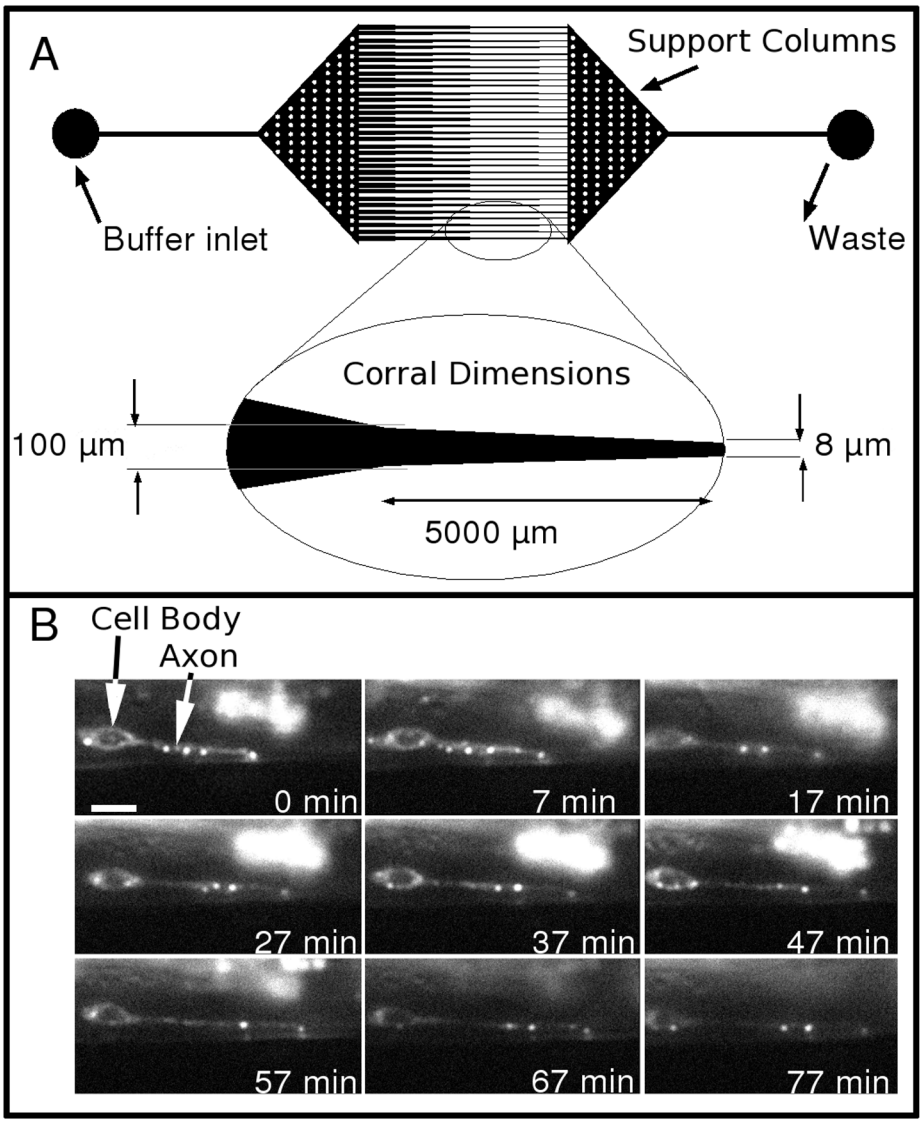

Figure 2.

Details of the worm corral and sample data. (A) A CAD drawing of the photomask used to generate the master for the microfluidic chip. The inlet and outlet regions have circular posts (white dots) to prevent the elastomeric chip from collapsing. Inset below the CAD drawing shows details of the dimensions of the finely tapered region. (B) A series of fluorescence images from a time-lapse series showing the early development of the HSNL motor neuron expressing GFP::RAB-3 in a L4 stage worm immobilized in the microchannel. The animal was rotated onto its side in this image so the bend in the axon was along the Z axis. The scale bar in the 0 min frame represents 3 µm.

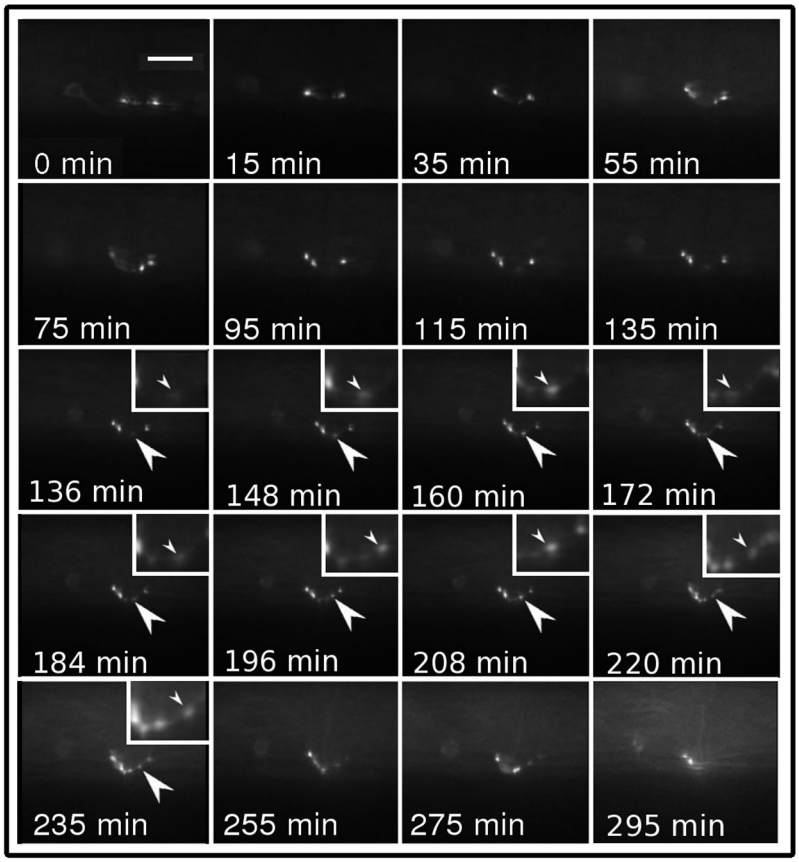

Figure 3.
A series of fluorescence time-lapse images showing the development of the HSNL motor neuron expressing GFP::RAB-3 in a YA worm. The series shows the established morphology typical at the end of the L4 stage progress to a mature synapse pattern. In the full animated sequence, movement of material between the puncta is visible and no ectopic synapses can be seen to develop. The scale bar in the 0 min frame represents 6 μm.

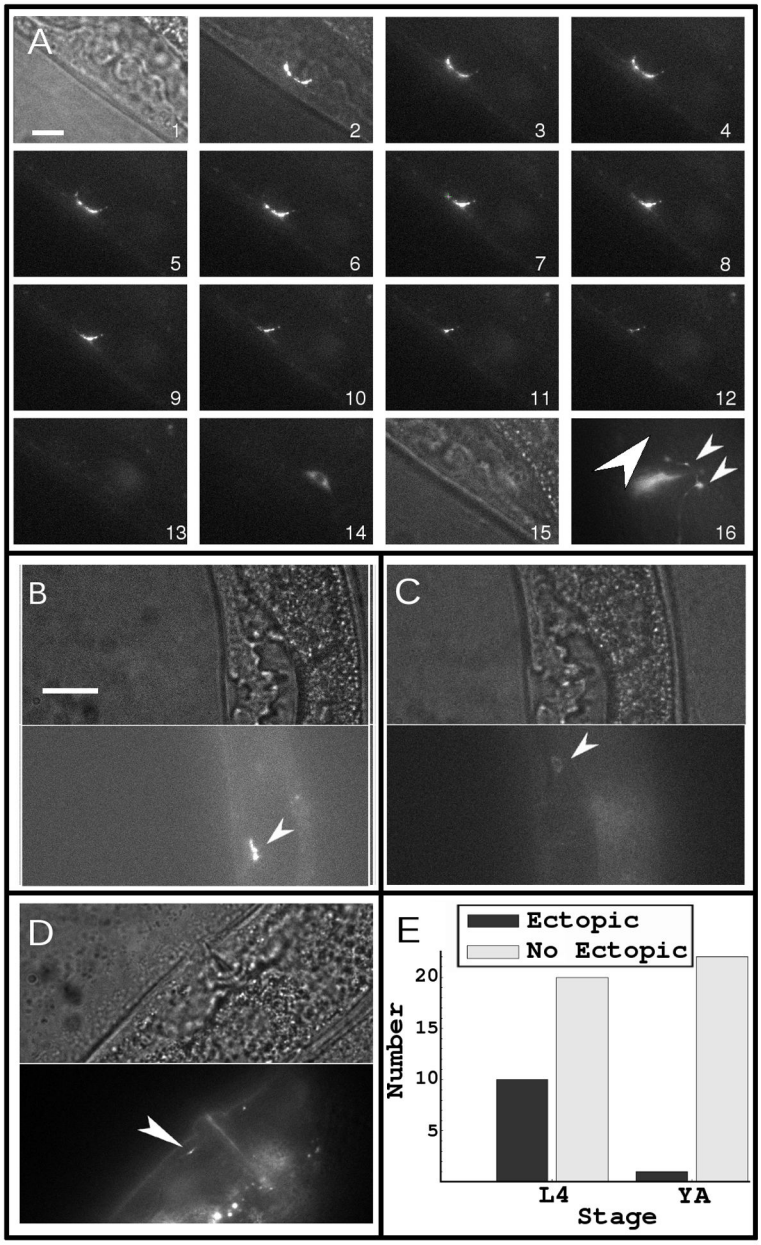

Figure 4.

The results of the ablation experiments. (A) A sequence of images showing the ablation of a mature synapse made by the HSNL neuron. Because the size of this synapse was much larger than the focal spot of the UV laser, we typically had to use more than ten pulses to ablate the entire synapse. Frame 1 is a bright-field image and frame 2 is a merged bright-field and fluorescence image prior to the ablation of the synapse. Frames 3–13 show the synapse during ablation. Frame 14 shows the cell body, which was out of focus in frames 3–13. Frame 15 is a bright-field image of the region where the ablated synapse was, which showed no overt damage to the specimen. Frame 16 shows the same specimen as in frame 13 and 15, but after development for several hours, during which the synapses reappeared (small arrows). The large arrow points to the region where an ectopic synapse would have formed, which in this case did not. (B) shows another specimen at an earlier stage of development in bright field (top panel)

and fluorescence (bottom panel) prior to ablation (the arrow indicates synaptic puncta). (C) shows the same specimen as in (B) after ablation in bright field (top panel) and fluorescence (bottom panel); the cell body can be seen in the fluorescence image and no overt damage is seen in the bright-field image (the arrow points to the cell body). (D) shows the same specimen as in (B) and (C) but after ablation and growth for several hours, after which an ectopic synapse had developed (arrow). (E) summarizes the results of 53 such experiments, which indicate ectopic synapses appear in worms in early developmental stage (L4) but not in YA worms. All scale bars represent 6 μm.